Int. J. Heat Mass Transfer. Vol. 20, pp. 911–918. Pergamon Press 1977. Printed in Great Britain

FLUIDISED BED COMBUSTION FOR THE STIRLING ENGINE

R. H. THRING
Engineering and Cybernetics Department, Reading University, Berkshire, England

(*Received* 1 *July* 1976 *and in revised form* 10 *November* 1976)

Abstract—Fluidised bed combustion is a possible method of providing the heat source for a Stirling engine, because it is near isothermal, low temperature (850–1100°C) and has a high heat-transfer coefficient. This paper presents theoretical models and experimental evidence of the heat-transfer coefficients expected in such an application, which are in the range 400–750 W/m² K.

NOMENCLATURE

A, tube area;
A_b, cross-sectional area of the bed;
Ar, Archimedes number, $Ar = \frac{g d_p^3}{\nu_g^2} \frac{\rho_s - \rho_g}{\rho_g}$;
C_{p_e}, specific heat of the emulsion packet;
C_{p_s}, specific heat of the solid;
d_p, mean particle diameter;
$\frac{dQ}{dx}$, rate of change of heat transfer to the heat pipe with respect to the distance below the datum;
d_s, inter-particle spacing;
F_e, view factor, assumed equal to unity;
f_0, bubble fraction;
g, acceleration due to gravity;
G_{mf}, mass velocity for minimum fluidisation;
h, heat-transfer coefficient;
H_f, bed depth at operating velocity;
H_{mf}, bed depth at minimum fluidisation;
h_r, radiative heat-transfer coefficient;
k_e, thermal conductivity of the emulsion packet;
k_s, thermal conductivity of the solid;
l_e, emulsion packet thickness;
l_g, gas gap thickness;
m_b, mass of bed;
Nu, Nusselt number, based on mean particle diameter;
q_r, radiative heat flux per unit area;
t, time;
T, temperature;
Tb, bulk bed temperature;
t_r, residence time of the emulsion packet at the heat-transfer surface;
T_w, heat-transfer surface temperature;
U_f, superficial fluidising velocity;
U_{mf}, minimum superficial fluidising velocity;
U_{opt}, fluidising velocity for maximum heat-transfer coefficient;
x, distance from heat-transfer surface.

Greek symbols

ΔT, temperature difference;
ε, emissivity;
ε_{mf}, bed voidage at minimum fluidisation;
λ, sphericity (= 1 for a sphere);
μ_g, gas viscosity;
ν_g, kinematic viscosity of the gas;
ρ_e, density of the emulsion packet;
ρ_g, gas density;
ρ_s, solid density;
σ, Stefan–Boltzmann constant.

1. INTRODUCTION

AS PART of a research effort aimed at the use of the fluidised bed combustor as a source of heat for the Stirling engine, it was found to be necessary to develop improved models of the heat-transfer process that occurs between a fluidised bed and an immersed surface and to back these up with experimental evidence. The reason for this is that the heat-transfer coefficients obtainable are functions of both the bed temperature and the heat-transfer surface temperature, and the experimental and theoretical results in the literature apply only to situations of relatively low heat-transfer surface temperature. In a Stirling engine application, the temperature of the heat-transfer surface is of the order of 700°C, and at this temperature the radiative contribution to heat transfer is expected to be large [1, 2]. The fact that existing heat-transfer models take only a rudimentary account of radiation heat transfer is, therefore, an added incentive to the production of improved models.

2. THEORETICAL MODELS

2.1. *Formulation*

Three models of heat transfer are presented here. All the models have a common macro-mechanism of heat transfer; that is, an "emulsion packet" consisting of particles and gas migrates from the centre of the bed to reside at the heat-transfer surface for a "residence

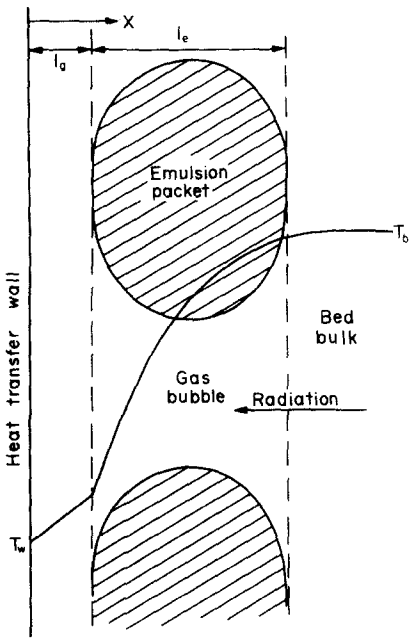

FIG. 1. Physical picture of the theoretical models.

time", and then returns to the bulk of the bed (see Fig. 1). During the residence time the emulsion packet is separated from the heat-transfer surface by a gas gap. Heat transfer occurs by the transient cooling (or heating) of the emulsion packet by (a) conduction and radiation through the packets themselves and thence across the gas-gap, and (b) by radiation alone through the bubbles (see Fig. 1). The micro-mechanism of heat transfer is the difference between the models. In model (1), the "packet model", the emulsion packets consist of a material of uniform thermal properties equal in magnitude to those of the unfluidised bed. This is a development of the type three theory (according to the classification of Gelperin and Einstein [2]), and as originally proposed by Mickley *et al.* [3]. Radiation is allowed for according to the simplistic approach of Vedamurthy and Sastri [6], by considering the emulsion packet to consist of a number of heat shields, through which the heat is transferred by absorption and re-radiation. The drawbacks of this model are (1) the emulsion packets cannot reasonably be considered to have uniform thermal properties, since the entire temperature gradient turns out to occur in the first few particle diameters away from the heat-transfer surface and (2) the radiation situation is evidently somewhat at variance with practice, since in reality the shields consist of particles and therefore have holes in them.

Models (2) and (3), the "spherical particle model" and the "cubical particle model" are a development of the type four theory [2], and as originally proposed by Botterill and Williams [4]. These models have the same macro-mechanism of heat transfer as the previous one, but now the emulsion packets are considered to consist of individual particles packed in such a way that the packet density equals the unfluidised bed density. The interstices are filled with the fluidising gas. The particles are either spherical or cubical, and practical results might be expected to lie between the two, except for particles of low sphericity, that is, needle-like particles. Heat transfer occurs by the transient cooling of the emulsion packets by (a) conduction through the particles, (b) radiation and conduction in the gaps between the particles and the gas-gap between the emulsion packet and the heat-transfer surface, and (c) by radiation alone in the bubbles.

The mathematical treatment of the models involved a transient numerical solution of a modified form of the diffusion equation for model (1) (equation 1), and a transient numerical solution of the normal diffusion equation coupled with non-steady radiation heat transfer for model (2) (equation 2). The results were time averaged as shown in Fig. 2 to give average values of heat-transfer coefficient.

$$\rho_e C_{p_e} \frac{\delta T}{\delta t} = k_e \frac{\delta^2 T}{\delta x^2} + \frac{\delta}{\delta x}(q_r) \tag{1}$$

where $q_r = \sigma F_e (T^4 - T_w^4)$

F_e = view factor, assumed unity

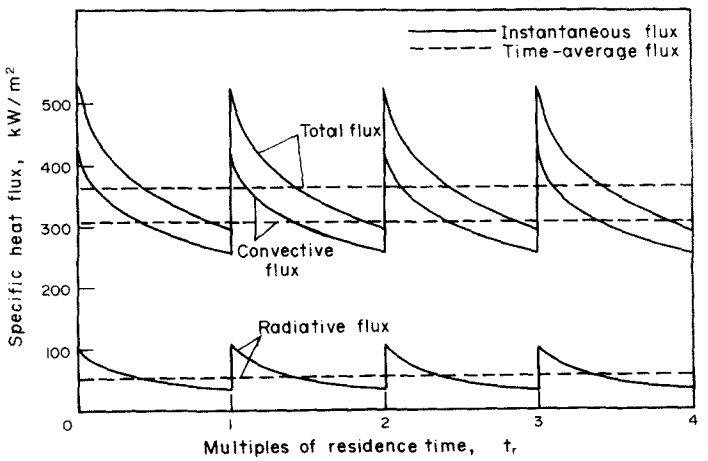

FIG. 2. Variation of heat flux with time. Cubical particle model. Superficial gas velocity = optimum; mean particle diameter = 1000 μm; bed temperature = 900°C; heat-transfer surface temperature = 30°C.

boundary conditions:

$$\text{at } t = 0,\ T = T_b \text{ for all } x \geqslant l_g$$

$$\text{at } x = l_g + l_e,\ T = T_b \text{ for all } t \geqslant 0$$

$$\rho_s C_{p_s} \frac{\delta T}{\delta t} = k_s \frac{\delta^2 T}{\delta x^2} \qquad (2)$$

boundary conditions:

$$\text{at } t = 0,\ T = T_b \text{ for all } x \geqslant l_g$$

$$\text{at } x = l_g + d_p + d_s,\ T = T_b \text{ for all } t \geqslant 0.$$

The complete mathematical treatment and computer programmes for the three models are published in [11].

The thickness of the emulsion packet was initially assumed to be equal to $3d_p$, and results confirmed that this was adequate, i.e. that at a distance of less than $l_g + 3d_p$ from the heat transfer wall the emulsion packet temperature at the end of the residence time was practically equivalent to the bed bulk temperature (see Fig. 3). The gas gap thickness was not assumed to be an arbitrary value as is often done [2, 6, 7] but was inserted into the final computer programme as a variable and the best value obtained. This is the only variable in the model that could not be obtained by independent experiment or calculation. The value used was $l_g = 0.08d_p$, and this was found to give satisfactory performance under all conditions.

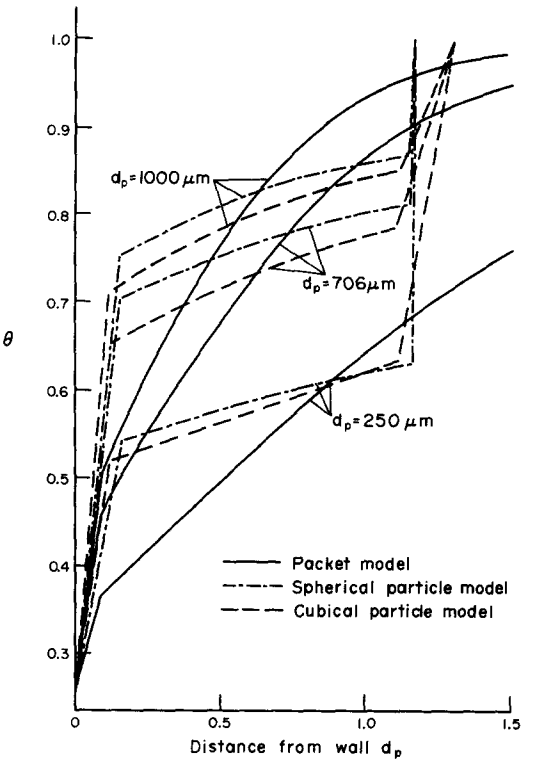

FIG. 3. θ vs distance at the end of the residence time. $T_B = 900°C$; $T_w = 30°C$; $U_f = U_{opt}$.

2.2. *Bed parameter correlations*

Since the heat-transfer mechanism depends on transient heat transfer during a residence time, the thermal properties of the materials and the residence time itself are important factors affecting heat transfer. There is some discrepancy in the values for residence time given in the literature; for example, the values obtained by Baskakov *et al.* [5] and Vedamurthy and Sastri [6] are much lower under the same conditions than those obtained by Mickley *et al.* [3] and Broughton [7]. However since Mickley *et al.* give greater detail of their experimental procedure, and their results agree well with those of Broughton, it was decided to use these results, the discrepancy being accounted for by Baskakov *et al.* having taken account of the smaller more rapid fluctuations in heat flux which occur during the residence time as observed by Mickley *et al.* These results are correlated by equation (3).

$$t_r = 8.932 \left[\frac{d_p g}{U_{mf}^2 \left(\frac{U_f}{U_{mf}} - 1 \right)^2} \right]^{0.0756} \left(\frac{d_p}{0.0254} \right)^{0.5} \qquad (3)$$

This correlation was used for all the models.

The fraction of the heat-transfer surface area that is exposed to bubbles is also important to the heat transfer. This can be found by experimental measurements of the bed depth since:

$$f_0 = 1 - \frac{H_{mf}}{H_f} \qquad (4)$$

as stated by Gelperin and Einstein [2]. Some experiments were carried out to correlate the bubble fraction with the main fluidising parameters and the result is given in equation (5).

$$f_0 = 0.08553 \left[\frac{U_{mf}^2 \left(\frac{U_f}{U_{mf}} - 1 \right)^2}{d_p g} \right]^{0.1948} \qquad (5)$$

The remaining bed parameter correlations are listed in Appendix 1.

2.3. *Results*

Figure 3 shows values of non dimensional temperature at the end of the residence time. The difference between the packet model and the particle model can be clearly seen. The figure emphasises the greater reality of models (2) and (3), since in practice there are bound to be sudden changes in the temperature gradient at the solid–gas interfaces. Figure 4 shows the variation of instantaneous specific heat flux with the time of contact of the emulsion packet, measured from the moment the packet arrived from the bulk of the bed. It can be seen that the radiative flux is much greater with models (2) and (3) than with model (1). This is because with models (2) and (3) the radiative heat flux is calculated from the surface temperature of the particles facing the heat-transfer surface, while model (1) assumes an arbitrary number of radiation shields exist across the packet. Figures 5 and 6 show the variation of heat-transfer coefficient with heat-transfer surface temperature, for models (1) and (2). Model (3) is very similar to model (2) here. The convective coefficient decreases with wall temperature because increasing the temperature of the heat-transfer

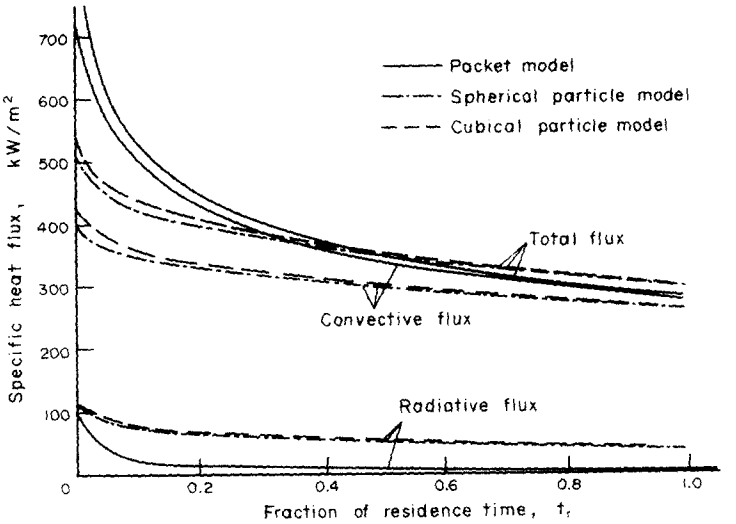

FIG. 4. Variation of instantaneous heat flux with residence time. $d_p = 1000\,\mu m$; $U_f = U_{opt}$; $T_B = 900°C$; $T_w = 30°C$.

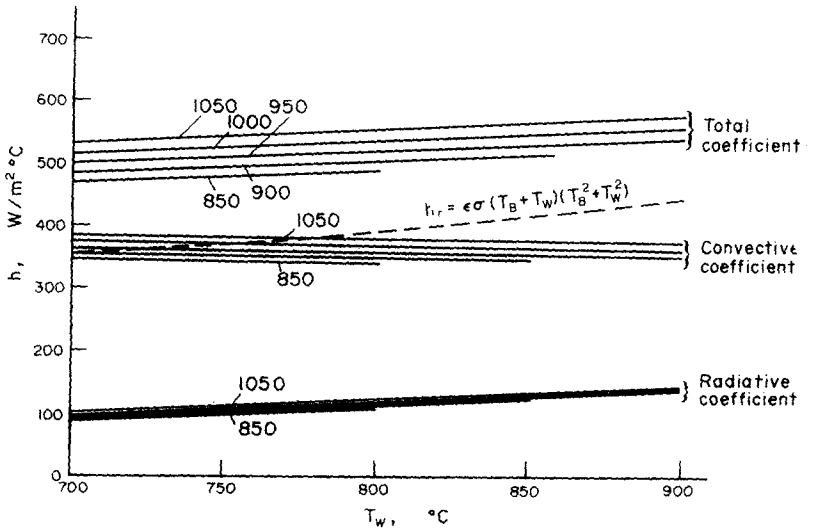

FIG. 5. Heat-transfer coefficient vs heat-transfer surface temperature for various bed temperatures. $d_p = 1000\,\mu m$; $U_f = U_{opt}$; packet model.

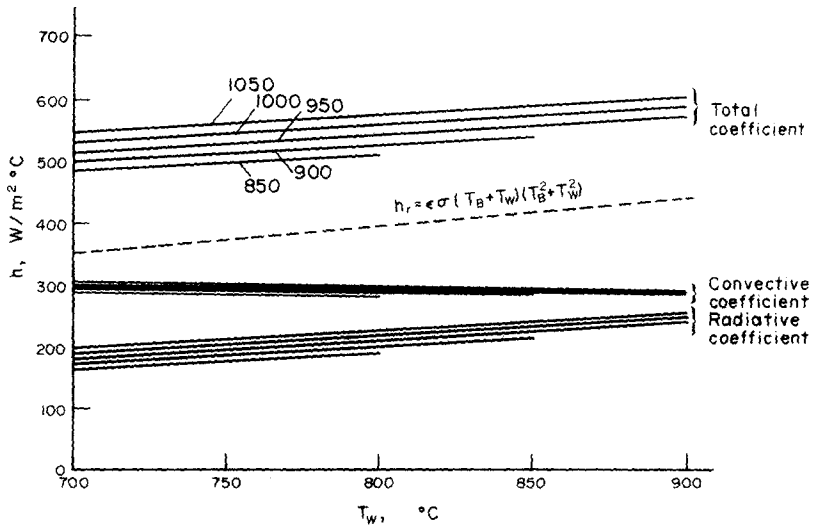

FIG. 6. Heat-transfer coefficient vs heat-transfer surface temperature for various bed temperature $d_p = 1000\,\mu m$; $U_f = U_{opt}$; spherical particle model.

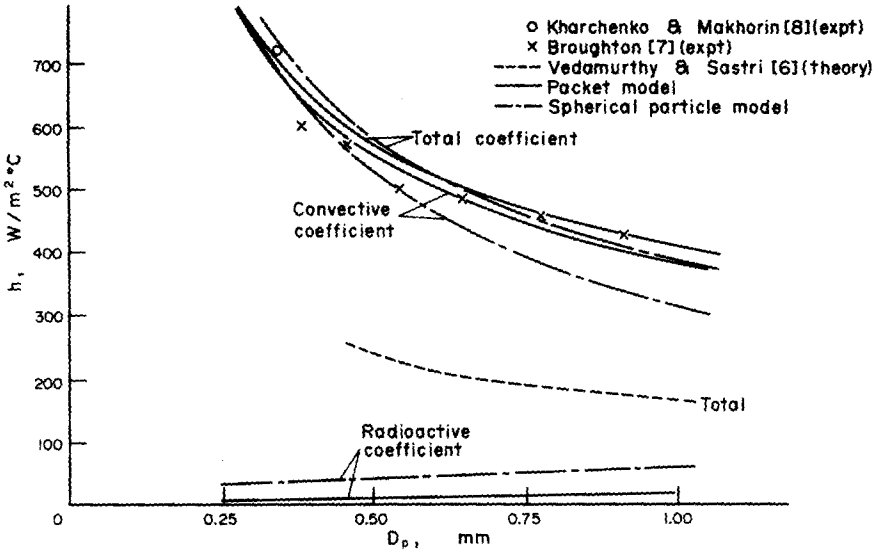

FIG. 7. Maximum h vs particle diameter, experimental and theory. $T_B = 900°C$; $T_w = 30°C$; material: sand.

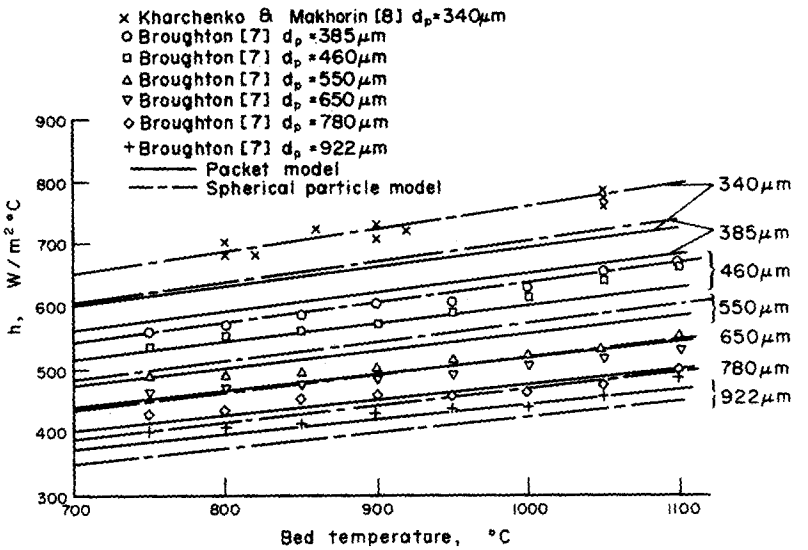

FIG. 8. Maximum total heat-transfer coefficient vs bed temperature.

surface decreases the amount by which the emulsion packet can cool off during the residence time, but the radiative coefficient can go on increasing because it is a function of the transfer surface temperature. In a simple approach to radiative heat transfer, Elliot *et al.* [1] give some values of radiative heat transfer calculated from:

$$h_r = \frac{\varepsilon\sigma(T^4 - t^4)}{\Delta t} = \varepsilon\sigma(T+t)(T^2+t^2). \qquad (6)$$

which is simply an adaptation of Stefan's black body radiation law. These values are also plotted on the figures and it can be seen that there is a considerable discrepancy. This is because in practice there is a shielding effect of the particles as they cool off during their residence time at the heat-transfer surface. When total heat-transfer coefficient was plotted as a function of superficial gas velocity for models (1) and (2), and compared with the experimental results of Kharchenko and Makhorin [8] and Broughton [7], it was found that model (2) predicted the results more closely than model (1).

Figure 7 shows heat-transfer coefficient vs particle size for models (1) and (2). Also shown is the result of the model of Vedamurthy and Sastri [6] which is the best model of this type so far produced. It can be seen that the new models give much better correlation than has been obtained previously. Figure 8 shows total heat-transfer coefficient vs bed temperature for various mean particle sizes as predicted by models (1) and (2). Also plotted in the figure are the results of Kharchenko and Makhorin [8] and Broughton [7] under the same conditions for comparison.

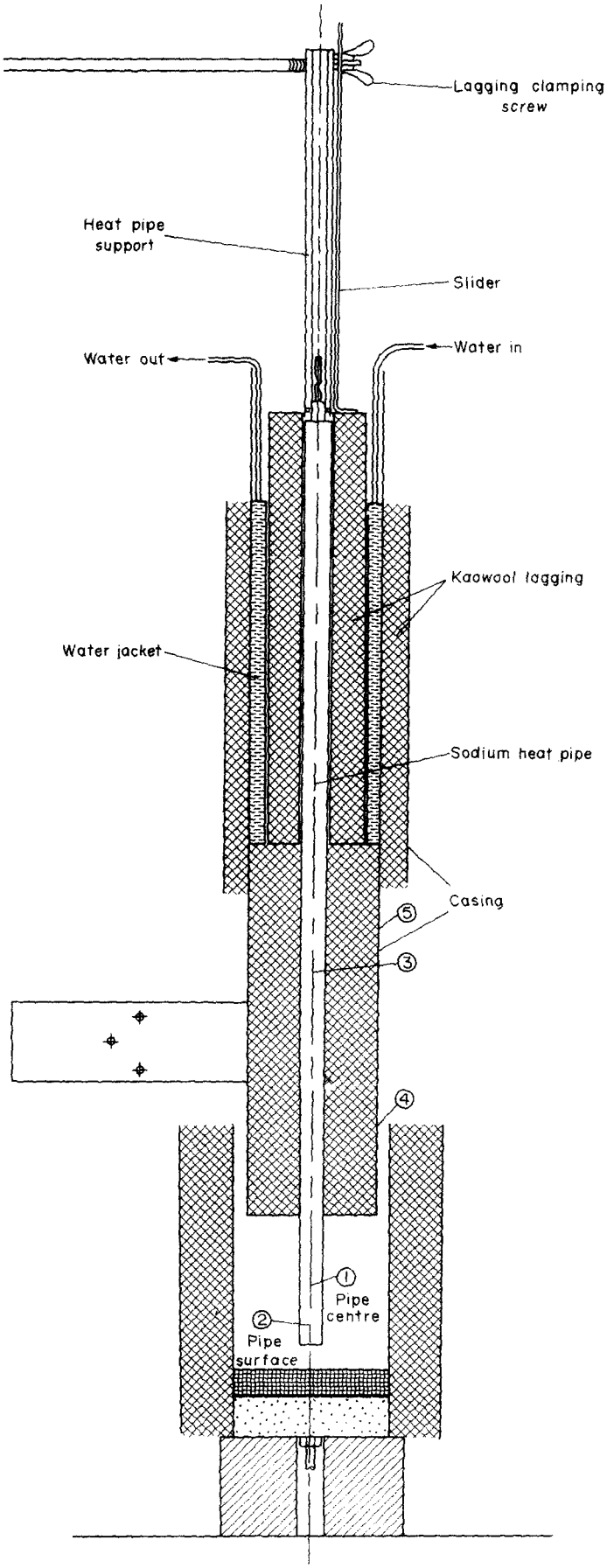

FIG. 9. Heat pipe measurement device. Scale 0.39 cm: 1 in. ⓝ = thermocouple.

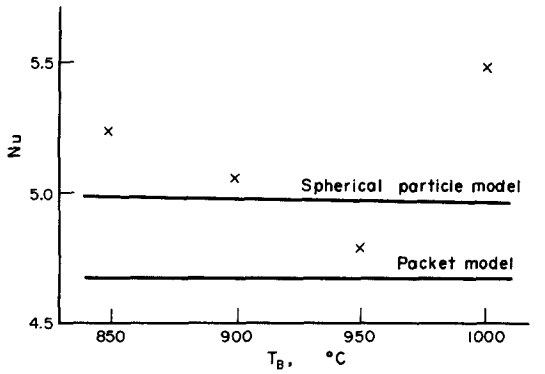

FIG. 10. Nusselt number vs bed temperature. Heat pipe temperature = 750°C; superficial gas velocity = 0.463 m/s; mean particle diameter = 582 μm.

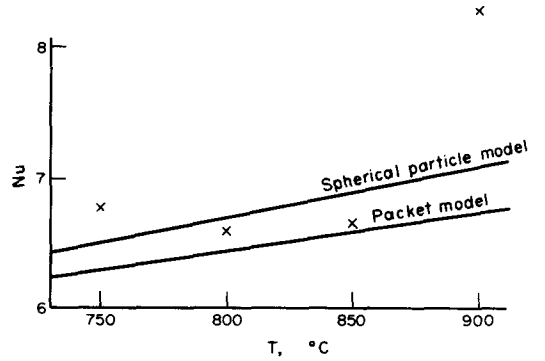

FIG. 11. Nusselt number vs heat pipe temperature. Bed temperature = 1000°C; superficial gas velocity = 0.675 m/s; mean particle size = 928 μm.

3. EXPERIMENTAL RESULTS

In order to confirm the predictions of heat transfer under Stirling engine conditions of the theoretical models, some experimental measurements of heat transfer were undertaken. The fluidised bed used was a 150 mm dia propane burning bed of sand particles, see Fig. 9. For making heat-transfer measurements, the method adopted is similar to that of Broughton [7], except that where he used a water cooled probe, here the heat-transfer surface had to be at 750–900°C, and so a sodium in stainless steel heat pipe was used. The principle of the method is that starting from a datum point, the cylindrical heat pipe is lowered vertically into the bed, increasing the cooling to keep the heat pipe temperature constant. A plot is made of the heat flux through the heat pipe vs the depth below the datum. The gradient of this line is dQ/dx, and since:

$$Q = AhΔT \tag{7}$$

or

$$\frac{dQ}{dx} = \frac{dAhΔT}{dx} \tag{8}$$

the heat-transfer coefficient, h, can be determined. The condenser end of the heat pipe was cooled by a novel type of calorimeter (Fig. 9). This was necessary because of the large range of total heat flux required, and the need to avoid freezing of the sodium in the condenser. The condenser section was surrounded by an annular space several centimetres thick, around which there was a cylindrical water cooled jacket coated on the inside with optical matt black. The heat transfer was by convection and radiation across the gap. For regulating the heat flow, a cylindrical jacket containing a thermal insulator could be inserted the required distance into the annular gap.

The results obtained from this apparatus are shown in Figs. 10–12. The estimated maximum experimental error in these results is 10%. The Nusselt number is based on particulate diameter. Also shown are the predictions of models (1) and (2), model (3) being similar to model (2). The results are somewhat scattered because they apply to a much smaller temperature difference than in the literature, so that the same error in specific heat flux produces a much larger error in heat-transfer coefficient. It was found that the Nusselt number increased linearly with particle size over the range covered, while the bed temperature has little effect (Fig. 10). Nusselt number increases linearly with the heat-transfer surface temperature (Fig. 11). Figure 12 shows Nusselt number vs Archimedes number.

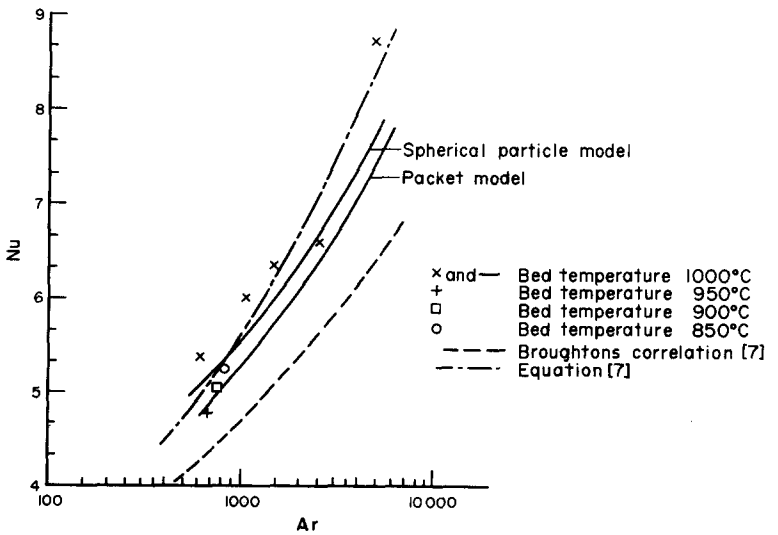

FIG. 12. Nusselt number vs Archimedes number.

Over the range covered the data can be correlated by:

$$Nu = Ar^{1/4}. \quad (9)$$

Also shown in the figure is Broughton's [7] correlation for heat transfer to water cooled surfaces. The increase in Nusselt number caused by the high temperature heat-transfer surface is clearly visible.

4. CONCLUSIONS

The results of three different models of heat transfer in fluidised beds show that the type of model used makes a large difference (of the order of a factor of two) to the predicted values of radiative coefficient obtainable between a fluidised bed and a heat-transfer surface. However, the results are always much less than the values predicted by assuming direct radiation from the bed at its mean temperature to the heat-transfer surface.

The predicted temperature profiles at the bed/surface interface suggest that models based upon consideration of individual particles are much more realistic than those based upon the mean thermal properties of the fluidised bed.

However, the agreement between the models and experimental results is similar for all the models, so that provided the split of total heat transfer into convective and radiative heat transfer is not important, either type of model could be used.

The experimental results using high temperature heat-transfer surfaces show that heat-transfer coefficients for the Stirling engine application can be obtained in the range 400–750 $W/m^2 K$. These results show good agreement with the theoretical predictions.

Acknowledgements– The author wishes to thank Professor P. D. Dunn and Dr. G. Rice of Reading University for their help and advice during the progress of this work. The work was supported by the Science Research Council.

REFERENCES

1. D. E. Elliott, E. M. Healey and A. G. Roberts, Fluidised bed heat exchangers, Heat Exchangers Conference, Institute of Fuel (1971).
2. N. I. Gelperin and V. G. Einstein, Heat transfer in fluidised beds, *Fluidisation*, edited by J. F. Davidson and D. Harrison, Chapter 10. Academic Press, New York (1971).
3. H. S. Mickley, D. S. Fairbanks and R. D. Hawthorn, The relation between the transfer coefficient and thermal fluctuations in fluidised bed heat transfer, *Chem. Engng Progr. Symp. Ser.* No. 57, **32**, 51 (1961).
4. J. S. M. Botterill and J. R. Williams, The mechanism of heat transfer to gas fluidised beds, *Trans. Instn Chem. Engrs* **41**, 217 (1963).
5. A. P. Baskakov, B. V. Berg, O. K. Vitt, N. F. Filippovsky, V. A. Kirakosyan, J. M. Goldobin and V. K. Maksaev, Heat transfer to objects immersed in fluidised beds, *Powder Technol.* **8**, 273–282 (1973).
6. V. N. Vedamurthy and V. M. K. Sastri, An analysis of the conductive and radiative heat transfer to the walls of fluidised bed combustors, *Int. J. Heat Mass Transfer* **17**, 1–9 (1974).
7. J. Broughton, Fluidised bed combustion, Ph.D. Thesis, University of Newcastle-upon-Tyne (August 1972).
8. N. V. Kharchenko and K. E. Makhorin, The rate of heat transfer between a fluidised bed and an immersed body at high temperatures, *Int. Chem. Engng* **4**(4), 650 (1964).
9. D. Kunii and O. Levenspiel, *Fluidisation Engineering*, pp. 265–301. John Wiley, New York (1969).
10. M. Leva, M. Weintraub, M. Grummer, M. Pollchick and H. H. Storch, Heat transmission through fluidised beds of fine particles, U.S. Bur. Mines Bulletin 504 (1951).
11. R. H. Thring, Fluidised bed combustion for the Stirling engine, Ph.D. Thesis, University of Reading (1975).

COMBUSTION EN LIT FLUIDISE POUR MOTEUR STIRLING

Résumé—La combustion en lit fluidisé est une méthode possible pour réaliser la source de chaleur d'un moteur Stirling, parce qu'elle est à peu près isotherme, à basse température (850–1100°C) et qu'elle a un grand coefficient de transfert thermique. Cet article présente des modèles théoriques et des résultats expérimentaux, de l'ordre de 400–750 $W/m^2 K$, pour le coefficient de transfert thermique attendu dans une telle application.

WIRBELBETTVERBRENNUNG FÜR STIRLING-MASCHINEN

Zusammenfassung—Eine mögliche Methode zur Beheizung von Stirling-Maschinen stellt die Wirbelbettverbrennung dar, da sie nahezu isotherm und bei niedrigen Temperaturen (850–1100°C) verläuft und hohe Wärmeübergangskoeffizienten aufweist. Es werden theoretische Modelle und Versuchsergebnisse für die bei dieser Anwendung auftretenden Wärmeübergangskoeffizienten angeführt; die Wärmeübergangskoeffizienten liegen dabei im Bereich von 400–750 $W/m^2 K$.

ГОРЕНИЕ В ПСЕВДООЖИЖЕННОМ СЛОЕ В ПРИМЕНЕНИИ К ДВИГАТЕЛЮ СТЕРЛИНГА

Аннотация — Горение в псевдоожиженном слое представляет потенциальный источник тепла для двигателя Стерлинга, т. к. процесс этот близок к изотермическому, происходит при низкой температуре (850–1100°C) и высоком коэффициенте теплообмена. В статье приводятся теоретические модели, а также экспериментальные коэффициенты теплообмена, которые в данном случае охватывают диапазон от 400 до 750 вт/м²К.